NANO LETTERS

pubs.acs.org/NanoLett

Plasmonic Activity of Large-Area Gold Nanodot Arrays on Arbitrary Substrates

Marisa Mäder,[†] Thomas Höche,*[,†] Jürgen W. Gerlach,[†] Susanne Perlt,[†] Jens Dorfmüller,[‡] Michael Saliba,[‡] Ralf Vogelgesang,[‡] Klaus Kern,[‡] and Bernd Rauschenbach[†]

[†]Leibniz Institute of Surface Modification, Permoserstrasse 15, D-04318 Leipzig, Germany, and
[‡]Max-Planck-Institute for Solid State Research, Heisenbergstrasse 1, D-70569 Stuttgart, Germany

ABSTRACT Highly efficient fabrication of well-ordered, embedded gold nanodot matrices using diffraction mask projection laser ablation is demonstrated. These gold nanodot arrays are ideally generated onto sapphire substrates but do also form onto AlO_x thin films, enabling the application to arbitrary bulk substrates. Well-ordered gold dots become embedded into the Al_2O_3 substrate during the process, thus improving their mechanical stability, chemical inertness, and technological compliance. Such substrates may be useful, for example, to enhance solar-cell efficiency by surface plasmons or as convenient, biocompatible focusing elements in nearfield optical tweezers.

KEYWORDS Metallic nanodots, surface plasmons, laser ablation

While the first theories describing the behavior of metal nanoparticles in the presence of an electromagnetic field were already developed in the early 20th century,[1,2] the topic gained new impact due to enhanced resolution in analytics and improved synthesis methods for nanoparticles. Especially the introduction of surface-enhanced Raman scattering (SERS) in the 1970s[3,4] proved a crucial milestone. Ever since then, the size- and shape-dependence of plasmon resonances in particles and the related absorption behavior,[5,6] the theoretical description of surface plasmon polaritons (SPPs),[7,8] and possible applications like light wave-guiding,[9−12] optical antennas,[13,14] optical nanocircuits,[15] efficiency enhancement of solar cells,[16,17] or even optical tweezers[18−21] have been attracting broad scientific and application interest.

Covering surfaces with metallic nanoparticles can enhance the coupling of light to interfaces. For example, by depositing gold nanoparticles onto the surface of a dielectric waveguide, Eurenius et al.[22] were able to access waveguide modes even under perpendicular excitation and with a disordered particle array. Often, the *k*-vector mismatch between light and plasmons that prohibits direct coupling is eluded by structuring the surface of the waveguides with regular gratings.[23] Recently, ideas to enhance coupling of light into solar cells by plasmonic nanostructures were reported.[16,17] Commercialization of the latter approaches will, however, critically depend on the ability to fabricate nanostructures in a reliable process on an industrial scale while making them durable at the same time.

In the present contribution, we prove that diffraction mask projection laser ablation (DiMPLA) is capable of generating well-ordered nanodot matrices bound to a sapphire substrate.[24] Furthermore, their potential use for plasmonic applications is demonstrated. It will be shown that gold nanodots are embedded in the dielectric substrate after fabrication, yielding high mechanical stability and chemical inertness. Referring to the solar cell architecture suggested by Ferry et al.[17] we propose similar results for efficiency enhancement with less effort and costs. Plasmonic activity of the gold dot matrix is confirmed experimentally by apertureless scanning near-field optical microscopy (aSNOM).

The fabrication of the nanodot arrays discussed here can be subdivided into two main steps. First, an ultrathin gold film is deposited onto a sapphire substrate, and second, this film is patterned by the laser top-down technique DiMPLA with a laterally varying intensity distribution. DiMPLA was earlier applied to synthesize GaN nanowires[25] and became later refined to generate rare-metal nanodot arrays.[26]

In the present contribution, gold dots on one type of substrate are reported on only, even though DiMPLA was proven to work for other metal−substrate combinations as well.[27] Onto c-plane and r-plane cut sapphire substrates, gold films were deposited by dc-magnetron sputtering at an argon gas pressure of about 1.0 Pa and a power of 30 W (deposition rates: ∼0.35 nm/s). The film thickness ranging between 5 and 10 nm was measured by X-ray reflectometry.

Patterning the gold film was done using a pulsed excimer laser featuring KrF as active lasing medium (wavelength λ = 248 nm, pulse duration λ = 25 ns). The laser is sent through a phase mask provoking distinct maxima of diffraction. The latter mask was fabricated by laser ablating resist from a plane-parallel fused silica plate and subsequent ion beam etching. By proper choice of structure depth, enhancement or suppression of individual orders of diffraction can be accomplished. For the work presented here, suppression

* Corresponding author, thomas.hoeche@iom-leipzig.de.
Received for review: 08/14/2009
Published on Web: 12/16/2009

DOI: 10.1021/nl903633z | *Nano Lett.* **2010,** *10,* 47-51

of the zeroth order of diffraction was desired because only the first order of diffraction can pass the aperture of the demagnifying objective following in the beam path. With a wavelength of 248 nm, the ideal height for the structures in the fused silica mask is 244 nm.[27] The actual height of mask structures employed here was about 270 nm due to unpredictabilities of the fabrication process. Only first orders of diffraction which possess enhanced intensity due to suppression of the zeroth order are then used for patterning by letting the laser light pass through a reflective objective. zeroth and second and all higher orders are blocked out of the subsequent beam path. Demagnified by the objective (×15), beamlets of the first order of diffraction are superimposed within the focal plane of the objective. The thin film, when positioned exactly in that focal plane, is then illuminated by an intensity pattern that possesses minima and maxima in the film plane.

During illumination with one single laser pulse, about 60% (the actual amount depends on fluence) of the Au film is ablated while the remaining gold melts and forms structures of minimized surface energy at the position of heat sinks. The formation process of the structures is proposed to be due to Marangoni convection. Temperature gradients lead to gradients in surface energy that eventually yield forces on the gold residues directed toward colder regions. Additionally, the surface of the substrate underneath the film melts for a short period of time and gold dots resolidify embedded into the substrate. This is because upon processing at high laser fluences (about 2 J/cm^2), the pristine gold layer becomes so hot (in excess of 2,500 K) that for a short time it exceeds the melting point of the sapphire substrate (2,327 K). By heat conduction, the sapphire surface melts, and in a liquid Al_2O_3 phase formed far off thermal equilibrium, the gold adopts the shape of dots that sink into the superficially molten sapphire minimizing their surface energy until extremely rapid solidification occurs.

Figure 1 shows a typical top-view scanning electron micrograph of a gold nanodot matrix. One of the main advantages of DiMPLA can be seen directly from this picture. With just one laser pulse of about 25 ns duration, very large areas in relation to size and periodicity of the structures can be fabricated.[24] Typical sizes of processed areas are 100 × 100 to 200 × 200 μm^2 while the diameter of the dots is typically 100−200 nm. The particular samples investigated further for this report were measured to feature nanodots of a mean diameter of 150 nm. The size was determined by measuring at least 100 dots from a scanning electron microscope micrograph and calculating the average. The transmission electron microscopy cross section (Figure 2) proves (i) the near-surface region of the substrate to be amorphous and (ii) the partial or complete embedding of gold spheres into sapphire.

The plasmon excitation on the gold dots is proven by near-field microscopy. The description of dipole excitation in spherical particles much smaller than the wavelength of

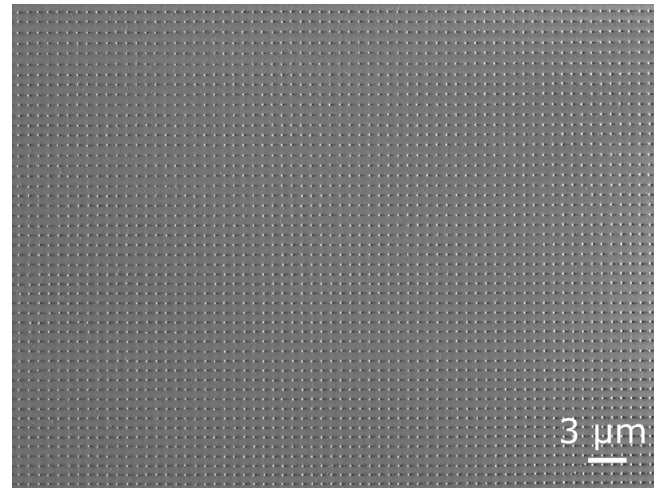

FIGURE 1. Typical top view of a large area gold nanodot matrix on a sapphire substrate made by DiMPLA.

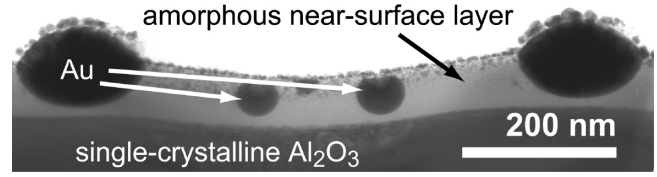

FIGURE 2. Transmission electron microscopy (TEM) cross section of two gold dots out of a row of well-ordered gold nanodots created with the DiMPLA technique. Clearly, the particles are embedded into an amorphous near-surface layer of the sapphire substrate. Presumably depending on laser fluence and roughness of the original gold film, the dots are enclosed either completely (small residues in the middle) or partly (larger dots at positions of intensity minima).

incident light was first given by Mie back in 1908.[1] The maximal extinction appears for the condition[7,8] $\varepsilon_1 = -2\varepsilon_m$, where $\varepsilon(\omega) = \varepsilon_1 + i\varepsilon_2$ is the frequency-dependent, complex dielectric function of the metal and ε_m is the dielectric constant of the dielectric medium. For the combination of gold and Al_2O_3, this condition is fulfilled at a wavelength of about 540 nm. For spheres with diameters in the range of 150 nm, however, a significant red shift would be expected.[28] Since the spheres produced with DiMPLA are not entirely covered by the substrate material, the effective dielectric constant of the surrounding medium is different than that of pure sapphire, resulting in a blue shift of the peak.

To make the surface plasmons on nanodots visible, apertureless scanning near-field optical microscopy (aSNOM) was used in a cross-polarization scheme.[29] In aSNOM, a laser beam (λ_{exc} = 942 nm) is mildly focused onto the sample under an oblique illumination angle (≈70° to the surface normal). The s-polarized light drives a plasmon excitation of the gold nanodots. The electromagnetic near-field pattern associated with this particle plasmon is probed with a commercial Si noncontact mode atomic force microscope (AFM) tip. The near-field component polarized perpendicular to the substrate surface is picked up by the tip and scattered into the far-field. An analyzer rotated to p-polarization is

DOI: 10.1021/nl903633z | *Nano Lett.* **2010,** *10,* 47-51

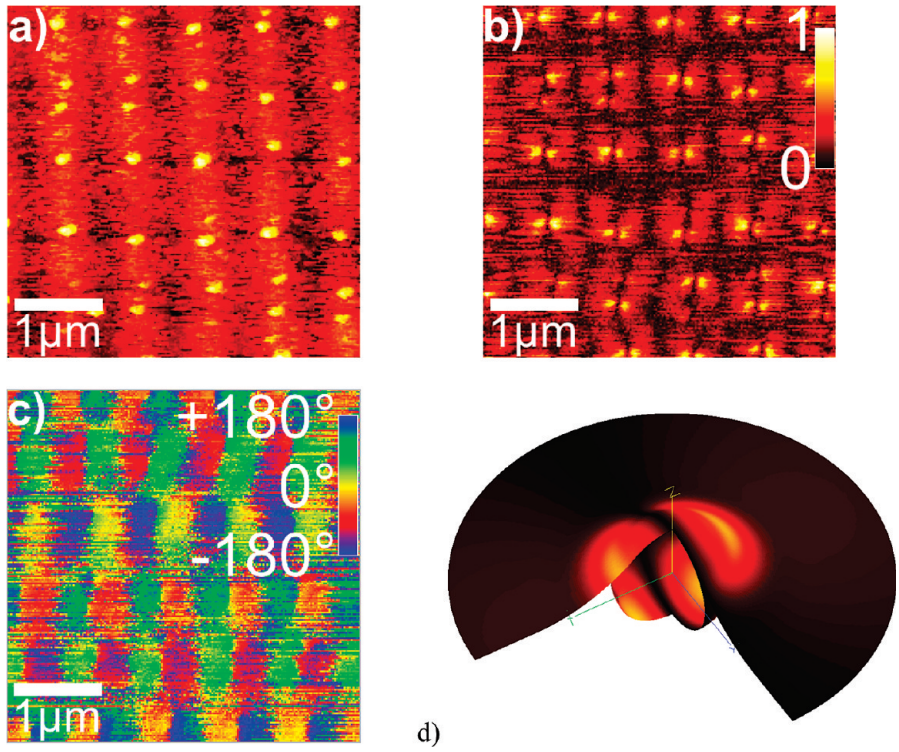

FIGURE 3. Apertureless SNOM measurements of a gold nanodot matrix created with DiMPLA. (a) The AFM topography signal. (b) The measured $|E_z|$ component above the same area as in (a). In a line-by-line correction a small complex valued offset has been subtracted. The optical signal clearly shows plasmonic dipoles at the corresponding positions of the nanospheres. (c) The corresponding phase image. The phase image underpins the dipolar character by indicating a phase difference of approximately 180° between the two lobes belonging to one particle. (d) Three-dimensional view (radius = 300 nm) of the simulated optical response of an isolated, semisubmersed Au sphere (radius = 84 nm). The quarter cutaway reveals the Au−sapphire and sapphire−air interface geometries. The same color scale as in (b) indicates the scattered $|E_z|$ component for $\lambda_{exc} = 942$ nm at normal incidence.

blocking the s-polarized light used for illumination, and demodulation at the second harmonic of the AFM cantilever vibration frequency allows the discrimination of the near-field signal.[30,31] Previous studies[29] have shown that the measured signal is in good agreement with the *z*-component of the *E*-field ≈20 nm above the structure as taken from simulations and that the perturbation of the near-field patterns by the tip is negligible.

The plasmonic excitation of the gold nanodots can be directly observed in aSNOM measurements. Figure 3a shows the AFM topography signal of the dot array. Panels b and c of Figure 3 depict simultaneously obtained optical signals, the amplitude and the phase, at an illumination wavelength of 942 nm. This wavelength is on the red side of the fundamental resonance, which suggests the predominant plasmonic response is dipolar in character. Correspondingly, the amplitude signal is dipole-like at positions of the associated nanodots. This finding is further accompanied by a phase difference of 180° between the two lobes of a particle, corroborating the expectation. Indeed, nearfield optical simulations (using the multiple-multipole platform MaX-1[32]) of Au spheres, semisubmersed in sapphire, confirm the

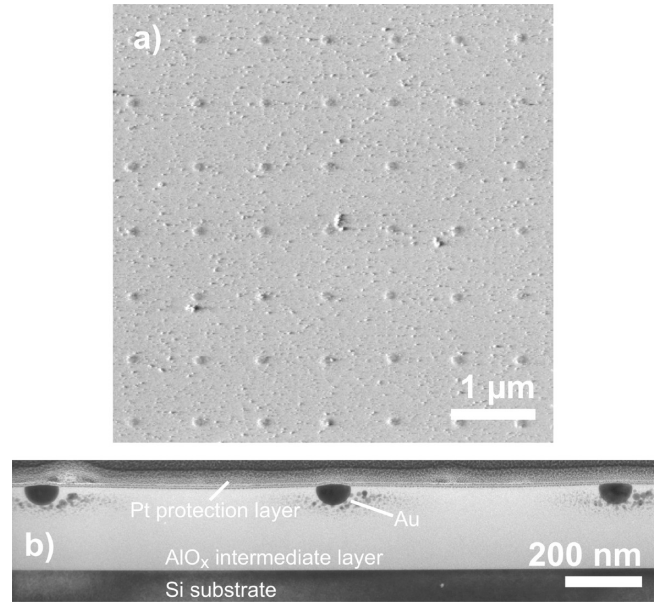

FIGURE 4. (a) SEM micrograph of DiMPLA-generated gold nanodots on a AlO_x intermediate layer on top of a silicon substrate. (b) TEM cross-sectional micrograph of a FIB-cut lamella of the sample shown in (a). The specimen was covered with a platinum protection layer prior to focused ion-beam processing.

DOI: 10.1021/nl903633z | *Nano Lett.* **2010,** *10,* 47-51

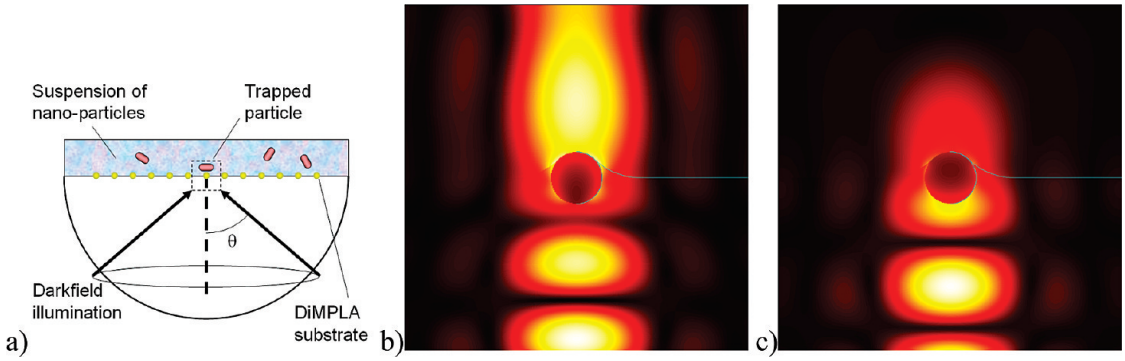

FIGURE 5. Nanotrapping with a DiMPLA substrate of optical tweezers. (a) Schematic of plasmon-assisted optical tweezing. (b) $1 \times 1\ \mu m^2$ overview of the total electric field distribution $|E|$ near a single Au sphere of radius 75 nm, semisubmersed in sapphire. H-polarized dark-field illumination of 532 nm excites the sphere from the sapphire side just above the critical angle for total internal reflection. Clearly, in the upper domain (assumed to be filled with water) a focal region is formed. (c) The same as (b), except for a slightly larger angle of excitation and subsequent loss of the optical tweezer focus.

measured field patterns at the accessible topside of the substrate and reveal details of the field distribution inside (Figure 3d).

As DiMPLA generation of Au nanodots on single-crystalline sapphire may be of limited use in certain applications, the question of using an intermediate layer to apply them to other substrates was also addressed. As shown in Figure 4, the generation of well-ordered gold nanodot arrays could be proven to work on a Si substrate this way. Like on bulk substrates before, the nanostructures become embedded in the layer (of about 220 nm thickness). A top-view scanning electron microscopy (SEM) micrograph is depicted in Figure 4a while Figure 4b shows a cross-sectional TEM micrograph of a focused ion beam-cut (FIB-cut) lamella of the same sample. The AlO_x layer was prepared using a high-pressure pulsed excimer laser deposition (PLD) technique.[33] It was found that for AlO_x layers possessing 90−300 nm thicknesses on Si substrates, well-ordered embedded gold nanodots were generated. Also on fused silica, Au nanodot arrays were successfully synthesized this way, suggesting that by deposition of an intermediate layer, DiMPLA-fabricated gold nanostructures can be applied to arbitrary substrates.

From the application point of view, this transferability of the straightforward laser pattering of Au films opens up new avenues in solar-cell design, as it has been shown earlier[17] that subwavelength scatterer positioned at the back of solar cells do significantly improve coupling of sunlight into the device. When built up onto a DiMPLA-patterned intermediate layer deposited onto a suitable substrate, ultrathin solar cells become feasible due to enhanced absorption mediated by the Au nanodot arrays. Furthermore, data storage in nanodot arrays consisting of magnetic alloys[34] onto low-thermal expansion substrates is another challenging application.

Another intriguing application of DiMPLA-patterned substrates may be plasmon-assisted optical tweezers (Figure 5a), which has been recently suggested.[18−21] The sapphire−gold combination is mechanically robust, chemically rather inert, and can be exposed to aqueous solutions. As it is also optically denser than water, (near-) total internal reflection may be used to limit exposure to a layer near the interface, and the embedded plasmonic Au spheres further enhance and laterally confine the light to a small focus volume in the solution. This should allow for convenient optical trapping and nanomanipulation of biological or medical nanoobjects in aqueous solutions. Our preliminary numerical results suggest that dark-field bottom illumination at angles slightly above the critical angle indeed results in a tightly focused volume of intense optical energy density above the Au sphere (Figure 5, panels b and c).

In summary, we report on a fast and straightforward method to create well-ordered embedded gold nanodots suitable for plasmonic applications. With DiMPLA, large-area gold nanodot matrices were generated, and with SEM and TEM it was proven that dots are embedded into the substrate, which guarantees high mechanical stability and chemical inertness. By aSNOM measurements, the plasmonic activity of the nanodot matrix is verified. Applications like efficiency enhancement of solar cells by attaching DiMPLA prepared structures to the backside of the cell utilizing an AlO_x intermediate layer or the usage of the embedded structures as optical traps are most feasible.

Acknowledgment. Financial support by a Deutsche Forschungsgemeinschaft grant (HO 1691/4-1) is gratefully acknowledged. Furthermore our thanks go to Helena Hilmer and Marius Grundmann (Leipzig University) who kindly provided the thin AlO_x films by PLD.

REFERENCES AND NOTES

(1) Mie, G. Beitrag zur Optik trüber Medien, speziell kolloidaler Metalllösungen. *Ann. Phys. (Leipzig)* **1908**, *25*, 377–445.
(2) Debye, P. Der Lichtdruck auf Kugeln von beliebigem Material. *Ann. Phys. (Leipzig)* **1909**, *30*, 57–136.
(3) Fleischmann, M.; Hendra, P. J.; McQuillan, A. J. Raman-Spectra of Pyridine Adsorbed at a Silver Electrode. *Chem. Phys. Lett.* **1974**, *26*, 163–166.
(4) Jeanmaire, D. L.; Van Duyne, R. P. Surface Raman Spectroelectrochemistry. 1. Heterocyclic, Aromatic, And Aliphatic-Amines Adsorbed On Anodized Silver Electrode. *J. Electroanal. Chem.* **1977**, *84*, 1–20.

DOI: 10.1021/nl903633z | *Nano Lett.* **2010,** *10,* 47-51

(5) Liz-Marzan, L. M. Nanometals: Formation and Color. *Mater. Today* **2004**, *7*, 26–31.
(6) Jensen, T.; Kelly, L.; Lazarides, A.; Schatz, G. C. Electrodynamics of noble metal nanoparticles and nanoparticle clusters. *J. Cluster Sci.* **1999**, *10*, 295–317.
(7) Zayats, A. V.; Smolyaninov, I. I.; Maradudin, A. A. Nano-optics of surface plasmon polaritons. *Phys. Rep.* **2005**, *408*, 131–314.
(8) Moores, A.; Goettmann, F. The plasmon band in noble metal nanoparticles: an introduction to theory and applications. *New J. Chem.* **2006**, *30*, 1121–1132.
(9) Genov, D. A.; Sarychev, A. K.; Shalaev, V. M.; Wei, A. Resonant field enhancements from metal nanoparticle arrays. *Nano Lett.* **2004**, *4*, 153–158.
(10) Barnes, W. L.; Dereux, A.; Ebbesen, T. W. Surface plasmon subwavelength optics. *Nature* **2003**, *424*, 824–830.
(11) Saj, W. M. FDTD Simulations of 2D plasmon waveguide on silver nanorods in hexagonal lattice. *Opt. Express* **2005**, *13*, 4818–4827.
(12) Brongersma, M. L.; Hartman, J. W.; Atwater, H. A. Electromagnetic energy transfer and switching in nanoparticle chain arrays below the diffraction limit. *Phys. Rev. B* **2000**, *62*, 16356–16359.
(13) Mühlschlegel, P.; Eisler, H.-J.; Martin, O. J. F.; Hecht, B.; Pohl, D. W. Resonant Optical Antennas. *Science* **2005**, *308*, 1607–1609.
(14) Greffet, J.-J. Nanoantennas for Light Emission. *Science* **2005**, *308*, 1561–1463.
(15) Huang, J.-S.; Feichtner, T.; Biagioni, P.; Hecht, B. Impedance Matching and Emission Properties of Nanoantennas in an Optical Nanocircuit. *Nano Lett.* **2009**, *9*, 1897–1902.
(16) Pillai, S.; Catchpole, K. R.; Trupke, T.; Green, M. A. Surface Plasmon enhanced silicon solar cells. *J. Appl. Phys.* **2007**, *101*, No. 093105.
(17) Ferry, V. E.; Sweatlock, L. A.; Pacifici, D.; Atwater, H. A. Plasmonic Nanostructure Design for Efficient Light Coupling into Solar Cells. *Nano Lett.* **2008**, *8*, 4391–4397.
(18) Righini, M.; Ghenuche, P.; Cherukulappurath, S.; Myroshnychenko, V.; Garcia de Abajo, F. J.; Quidant, R. Nano-optical Trapping of Rayleigh Particles and Escherichia coli Bacteria with Resonant Optical Antennas. *Nano Lett.* **2009**, *9*, 3387–3391.
(19) Righini, M.; Zelenina, A. S.; Girard, C.; Quidant, R. Parallel and selective trapping in a patterned plasmonic landscape. *Nat. Phys.* **2007**, *3*, 477–480.
(20) Miao, X.; Lin, L. Y. Trapping and Manipulation of Biological Particles Through a Plasmonic Platform. *IEEE J. Sel. Top. Quantum Electron.* **2007**, *13*, 1–8.
(21) Grigorenko, A. N.; Roberts, N. W.; Dickinson, M. R.; Zhang, Y. Nanometric optical tweezers based on nanostructured substrates. *Nat. Photonics* **2008**, *2*, 365–370.
(22) Eurenius, L.; Hägglund, C.; Olsson, E.; Keasmo, B.; Chakarov, D. Grating formation by metal-nanoparticle-mediated coupling of light into waveguided modes. *Nat. Photonics* **2008**, *1*, 1–5.
(23) Radko, I. P.; Bozhevolnyi, S. I.; Brucoli, G.; Martín-Moreno, L.; García-Vidal, F. J.; Boltasseva, A. Efficiency of local surface plasmon polariton excitation on ridges. *Phys. Rev. B* **2008**, *78*, 115115.
(24) Mäder, M.; Höche, T.; Gerlach, J. W.; Böhme, R.; Zimmer, K.; Rauschenbach, B. Large area metal dot matrices made by diffraction mask projection laser ablation. *Phys. Status Solidi RRL* **2008**, *2*, 34–36.
(25) Höche, T.; Böhme, R.; Gerlach, J. W.; Frost, F.; Zimmer, K.; Rauschenbach, B. Semiconductor nanowires prepared by diffraction-mask-projection excimer-laser patterning. *Nano Lett.* **2004**, *4*, 895–897.
(26) Höche, T.; Böhme, R.; Gerlach, J. W.; Rauschenbach, B.; Syrowatka, F. Nanoscale laser patterning of thin gold films. *Phil. Mag. Lett.* **2006**, *86*, 661–667.
(27) Mäder, M.; Zimmer, K.; Böhme, R.; Höche, T.; Gerlach, J. W.; Rauschenbach, B. Nano-Patterning by Diffraction Mask-Projection Laser Ablation. *J. Laser Micro/Nanoeng.* **2008**, *3*, 9–13.
(28) Link, S.; El-Sayed, M. A. Shape and size dependence of radiative, non-radiative and photothermal properties of gold nanocrystals. *Int. Rev. Phys. Chem.* **2000**, *19*, 409–453.
(29) Esteban, R.; Vogelgesang, R.; Dorfmüller, J.; Dmitriev, A.; Rockstuhl, C.; Etrich, C.; Kern, K. Direct Near-Field Optical Imaging of Higher Order Plasmonic Resonances. *Nano Lett.* **2008**, *8*, 3155–3159.
(30) Bek, A.; Vogelgesang, R.; Kern, K. Apertureless scanning near field optical microscope with sub-10 nm resolution. *Rev. Sci. Instrum.* **2006**, *77*, No. 043703.
(31) Vogelgesang, R.; Dorfmüller, J.; Esteban, R.; Weitz, R. T.; Dmitriev, A.; Kern, K. Plasmonic nanostructures in aperture-less scanning near-field optical microscopy (aSNOM). *Phys. Status Solidi B* **2008**, *245*, 2255–2260.
(32) Hafner, C. *Max-1: A Visual Electromagnetics Platform*; Wiley: Chichester, 1998.
(33) Lorenz, M.; Kaidashev, E. M.; Rahm, A.; Nobis, T.; Lenzner, J.; Wagner, G.; Spemann, D.; Hochmuth, H.; Grundmann, M. $Mg_xZn_{1-x}O$ ($0 \leq x < 0.2$) nanowire arrays on sapphire grown by high-pressure pulsed-laser deposition. *Appl. Phys. Lett.* **2005**, *86*, 143113.
(34) Parekh, V.; E, C. S.; Smith, D.; Ruiz, A.; Wolfe, J. C.; Ruchhoeft, P.; Svedberg, E.; Khizroev, S.; Litvinov, D. Fabrication of a high anisotropy nanoscale patterned magnetic recording medium for data storage applications. *Nanotechnology* **2006**, *17*, 2079–2082.

DOI: 10.1021/nl903633z | *Nano Lett.* **2010,** *10,* 47-51